Characterization of a novel series of highly selective PARP7 inhibitors

Cowley PM, McGuinness BE, Campbell GM and Wise A#

Duke Street Bio Ltd., 2 Duke St, London, UK

Abstract 486
AACR
2023

SCAN ME

Background

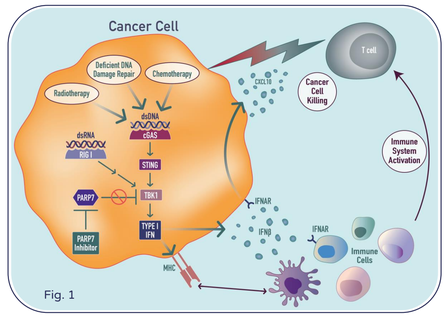

Fig. 1

PARP7 is a cellular stress-induced enzyme that adds mono-ADP-ribose groups to a variety of substrate proteins thereby regulating their function. One such substrate is the kinase TBK1 which regulates activity of cGAS-STING and RIG-I nucleic acid sensing pathways. Up-regulation of PARP7 expression in cancers applies a brake to cytosolic nucleic acid sensing and the Type I IFN response. This creates an immunosuppressive tumour microenvironment (TME) leading to faster tumour growth. Inhibition of PARP7 releases this brake, facilitating Type I IFN-driven immune activation (**Fig.1**). Inhibition of PARP7 has also been shown to directly arrest growth in a subset of cancer cells via the promotion of a senescence phenotype, inhibition of autophagy and regulation of metabolism. Using structure-based drug design we describe the characterization of potent and selective inhibitors of PARP7, exemplified by **DSB1148** .

In vitro Potency & ADME

Table 1. **DSB1148** is a potent PARP7 inhibitor in biochemical and cell-based assays, while also demonstrating excellent *in vitro* ADME.

Human *in vitro* potency & ADME		
PARP7 Binding	K_D (nM)	0.7
PARP7 nanoBRET	IC_{50} (nM)	0.8
MDA-MB-436 (BRCA1m)		
IFNβ Induction	IC_{50} (nM)	5
CXCL10 Induction		5
NCI-H1373		
5 Day Viability (Cell Titer Glo)	IC_{50} (nM)	19
14 Day Colony Forming Unit Inhibition		3.2
Liver Mics CLint (μL/min/mg) / Heps CLint (μL/min/10^6 cells)		8.4 / 4.4
Plasma Stability $T_{1/2}$ (mins) / Plasma Protein Binding (%)		>373 / 98.7
CYP Inhibition, 5 isoforms (μM)		>10
CYP Time-Dependent Inhibition (μM)		>10
Caco-2 (10^{-6} cm/s) A→B / Efflux Ratio		21.1 / 1.5

Table 2. **DSB1148** demonstrates excellent *in vivo* PK.

	Mouse	Rat	Dog
V_{ss} (L/kg)	0.74	2.12	1.61
IV CL (mL/min/kg)	11.33	38.69	3.02
IV $T_{1/2}$ (h)	0.75	0.77	6.07
Oral $T_{1/2}$ (h)	1.32	2.90	4.56
Oral Bioavailability (F%)	45.6	43.54	47.81

Fig. 2a

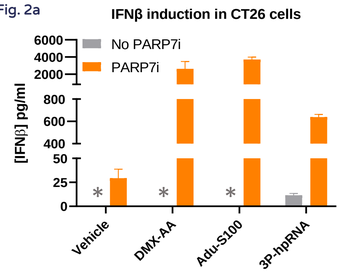

Fig. 2b

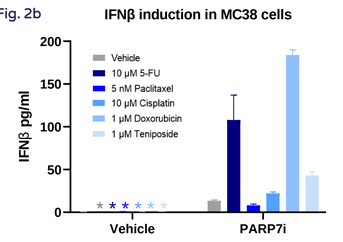

Fig. 2. **DSB PARP7i** work in concert with STING and RIG-I agonists (**Fig. 2a**) and DNA damaging agents (**Fig. 2b**) to induce Type I IFN. *Below limit of detection

Cell Line	Mutation	PARP7i Growth Arrest IC50 (nM)
NCI-H2122	**KRAS (G12C)**	**60 (partial)**
NCI-H23	**KRAS (G12C)**	**13**
NCI-H1373	**KRAS (G12C)**	**17**
Calu-1	**KRAS (G12C), EGFR Res**	**180 (partial)**
SW1573	**KRAS (G12C)**	**6239**
H358	**KRAS (G12C)**	**>10,000**
CAPAN II	**KRAS (G12V)**	**16**
H441	**KRAS (G12V)**	**5**
HCC1937	BRCA1 / PTEN Deficient	16
BT549	PTEN Deficient	5
A2780	-	3492
BT474	HER2	>10,000
JIMT1	HER2 Res	8644
MDA-MB-453	HER2 Res	6390
MDA-MB-157	XRCC1 deficient	1060
MM.1S	FGFR Res	189
A375	BRAF V600E	>10,000
A2058	BRAF V600E	2720
NCI-H1581	FGFR Act	>10,000
PC-9	EGFR Act	>10,000
NCI-H1975	EGFR Act	14

Table 3. **PARP7i** induce cGAS-STING independent growth arrest in a number of cancer cell lines.

Fig. 3

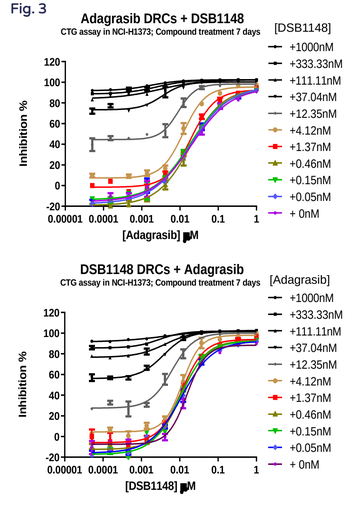

Figure 3. Combining **DSB1148** with KRAS G12C inhibitor yields additional *in vitro* efficacy.

In vivo efficacy

Fig. 4a

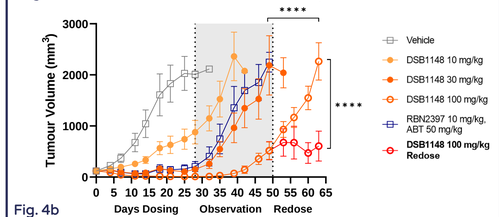

Fig. 4b

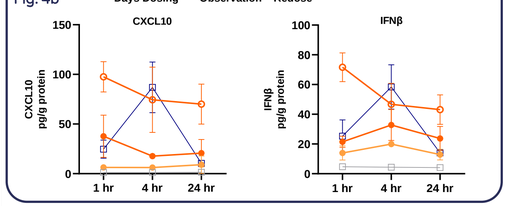

Fig. 4. **DSB1148** (p.o., BID) drives rapid tumour regression in a dose-dependent manner in an H1373 lung adenocarcinoma xenograft model (**Fig 4a**), which correlates with robust tumour PD (**Fig. 4b**).
****P<0.0001

Fig. 5a

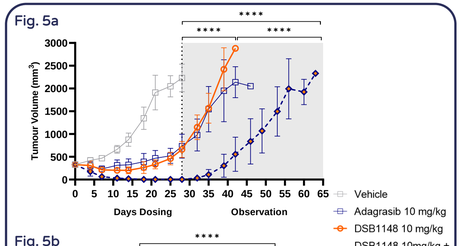

Fig. 5b

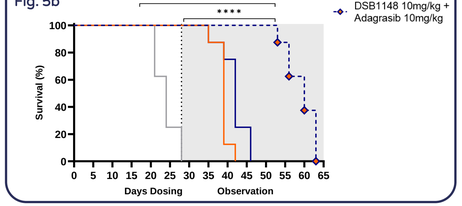

Fig. 5. A combination of **DSB1148** and KRAS G12C inhibitor Adagrasib, each at sub-efficacious dose levels, drives rapid and full tumour regression (**Fig. 5a**). Survival is also significantly prolonged vs either molecule alone (**Fig. 5b**).
****P<0.0001

Fig. 6a

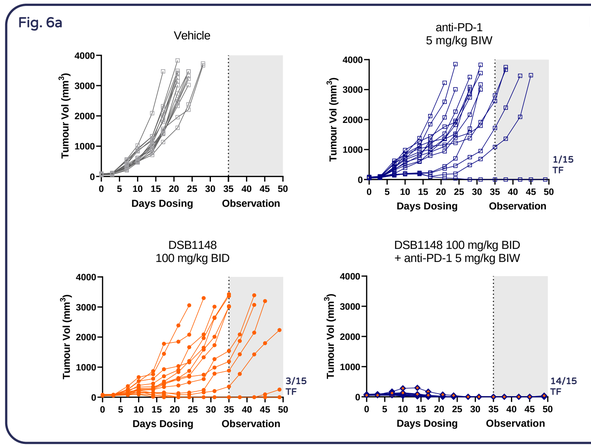

Fig. 6b

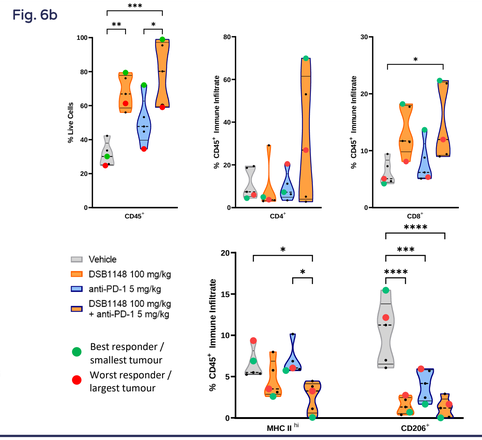

Fig. 6. **DSB1148** in combination with anti-PD-1 drives full tumour regression (100% mice tumour-free at 28 days of treatment) (**Fig. 6a**). Intra-tumoural immune cell infiltration was significantly increased in **DSB1148**-treated mice with evidence of elevated CD8+ and decreased CD4+ populations. Immune-suppressive M2 macrophages were significantly reduced following **DSB1148** treatment (**Fig. 6b**), suggesting that **DSB1148** facilitates establishment of an immune activated TME leading to tumour regression.
TF, tumour-free; *P<0.05; **P<0.01; ***P<0.001; ****P<0.0001.

Summary

We describe the characterization of a lead series of highly potent and selective PARP7 inhibitors which demonstrate excellent *in vitro* ADMET and *in vivo* PK properties leading to best-in-class anti-tumour efficacy in a KRAS-driven lung cancer xenograft model.

Our data support further studies investigating the use of PARP7 inhibitors in KRAS-driven cancers either as single agents or in combination with inhibitors of mutant KRAS. Our data also highlights the opportunity to utilise PARP7 inhibitors in cancers where high genomic instability leads to aberrant cytosolic nucleic acid levels or in concert with exogenous DNA-damaging agents.

Acknowledgements

Biochemical and nanoBRET assays were performed by Proteros Biostructures GmbH; *in vitro* biology, ADME and PK studies were carried out by BioDuro-Sundia; *in vivo* efficacy studies were conducted by BioDuro-Sundia and Crown Bioscience, Inc.

#Corresponding author

Alan Wise, PhD. CEO, Duke Street Bio Ltd.
awise@dukesb.com
www.dukestbio.com

LinkedIn